Comparison of the Hydration and Diffusion of Protons in Perfluorosulfonic Acid Membranes with Molecular Dynamics Simulations

Shengting Cui,* Junwu Liu, Myvizhi Esai Selvan, Stephen J. Paddison,* David J. Keffer, and Brian J. Edwards

Department of Chemical and Biomolecular Engineering, University of Tennessee, Knoxville, Tennessee, 37996-2200

Received: May 6, 2008; Revised Manuscript Received: August 11, 2008

Classical molecular dynamics (MD) simulations were performed to determine the hydrated morphology and hydronium ion diffusion coefficients in two different perfluorosulfonic acid (PFSA) membranes as functions of water content. The structural and transport properties of 1143 equivalent weight (EW) Nafion, with its relatively long perfluoroether side chains, are compared to the short-side-chain (SSC) PFSA ionomer at an EW of 977. The separation of the side chains was kept uniform in both ionomers consisting of $-(CF_2)_{15}-$ units in the backbone, and the degree of hydration was varied from 5 to 20 weight % water. The MD simulations indicated that the distribution of water clusters is more dispersed in the SSC ionomer, which leads to a more connected water-channel network at the low water contents. This suggests that the SSC ionomer may be more inclined to form sample-spanning aqueous domains through which transport of water and protons may occur. The diffusion coefficients for both hydronium ions and water molecules were calculated at hydration levels of 4.4, 6.4, 9.6, and 12.8 H_2O/SO_3H for each ionomer. When compared to experimental proton diffusion coefficients, this suggests that as the water content is increased the contribution of proton hopping to the overall proton diffusion increases.

Introduction

The polymer electrolyte in proton exchange membrane (PEM) fuel cells has been the focus of research aimed at improving the performance of the device to function under hot (i.e., >100 °C) and dry conditions.[1−3] Novel PEMs that possess good chemical and mechanical stability, low gas permeability, and high proton conductivity are needed, and the route to successful implementation into these power sources is tied to acquiring a systematic understanding of how proton mobility is determined by polymer structure and chemistry, water content, and choice of the protogenic group.[4] Some guidance may be inferred from what is understood concerning the transport of protons in bulk water: a combination of vehicular and structural diffusion processes, with the latter being the more dominant.[5−8] The regions of a hydrated PEM that contain the water, however, are exceedingly more complex than bulk water. The two diffusion mechanisms are thought to contribute to proton mobility in hydrated PEMs, but their relative contributions are not fully understood and are highly dependent on the water content and morphology of the membrane.[9]

Nafion, the archetypical PEM, is a perfluorosulfonic acid (PFSA) ionomer with pendant $-OCF_2CFCF_3OCF_2CF_2SO_3H$ side chains (see Figure 1a).When hydrated, this PFSA exhibits phase separation on a nanometer scale into regions consisting of the hydrophobic polytetrafluoroethylene (PTFE) backbone and domains consisting of tethered sulfonate groups, hydrated protons, and water molecules. Neutron diffraction studies have characterized the size of the water clusters in this aqueous phase to be of the order of 2−5 nm.[10] The morphology of the aqueous phase has been modeled as micelles of spherical water clusters,[11,12] layered structures,[13,14] polymer bundles,[15,16] or cylindrical channels.[17,18] The precise morphology of hydrated PFSA membranes is not definitively characterized despite extensive experimental and theoretical studies.[10,17,19−43] We refer to distinct portions of the aqueous region as clusters but do so without any implication as to the geometry. This terminology allows us to make contact with the percolation literature, in which the notion of a sample-spanning cluster (SaSC) is typical.

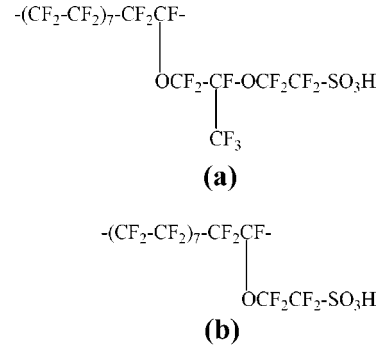

Figure 1. Chemical structures of the monomers used in the simulations with side chain separation of $-(CF_2)_{15}-$ in the PTFE backbone: (a) 1143 EW Nafion; (b) 977 EW SSC PFSA ionomer.

It is clear from percolation theory that there must be a sample-spanning cluster (SaSC) in order for there to be a net flux of species in a system with a static connectivity. If static aqueous phase morphology was present in a PFSA membrane, then there would have to be a sample-spanning aqueous region across the entire width of the material. However, in these electrolytes, the molecules undergo at least Brownian motion, resulting in relaxation of both the side chains and backbone of the polymer and the water molecules. This relaxation translates into a dynamic morphology which, along with vehicular and structural diffusion of protons, determines the proton conductivity of the

* Correspondence may be addressed to either author. E-mail: scui@utk.edu (S.C.); spaddison@utk.edu (S.J.P.).

10.1021/jp8039803 CCC: $40.75
Published on Web 10/01/2008

membrane. The time scale associated with the morphology relaxation is certainly larger than that associated with the diffusional processes. Vehicular diffusion occurring within a cluster may be estimated from molecular dynamics (MD) simulations, in which long-time behavior of the mean-square displacement (MSD) as a function of time is linear (as dictated by the Einstein relation), and on the order of 1−10 ns.[44] The proton hopping time is ∼1.5 ps and is significantly faster than the time associated with vehicular diffusion.[45,46] The time scale associated with the aqueous cluster dynamics is equivalent to the relaxation time of the polymer in the system because the two nanophases, together, are space-filling. It is more difficult to estimate the time scale associated with the relaxation of a polymer in a hydrated ionomer, but the typical time scale for a polymer is at least on the order of seconds.[47] Clearly, the time scale associated with aqueous cluster morphology dynamics is orders of magnitude slower than that for vehicular or structural diffusion of protons within a cluster.

We can conceive of a system in which protons move relatively rapidly within a cluster but are confined to remain within a given cluster until, on a longer time scale, "bridges" form between the clusters and the connectivity of the aqueous phase changes. Hence, the SaSC within the hydrated membrane consists of regions of dense aqueous clusters interconnected by irregular, less well-packed regions of water which act as channels. Efficient migration of protons through the membrane is therefore dependent on the existence of SaSCs. The morphology of hydrated membranes, as indicated earlier, is complex and irregular, and thus difficult to characterize through only a simple theory. Obviously, the morphology of the aqueous domains is influenced by the chemistry and crystallinity of the ionomer. Thus, a better understanding of the relationship between polymer architecture, along with the resulting hydrated morphology, will be critical for the development of novel high performance membranes.

A great variety of different PEMs have been synthesized[48,49] and characterized in an attempt to improve upon the unsatisfactory proton conductivity of Nafion at low water contents. These novel ionomers include the following: PFSA ionomers[50] with differing side chain, lengths and equivalent weights (EWs); nonfluorinated[51] aromatic polymers such as polysulfones, poly(ether ketones), poly(phosphazenes), and polyimides; composites[52,53] such as conventional ionomers containing silica, titania, heteropolyacids, layered metal phosphonates, etc. Although several of these materials show improvements over Nafion in certain respects, such as long-time thermal stability at $T > 130$ °C and conductivities that are quite a bit higher at very low water contents, no membrane has been developed that is superior in all respects and meets the requirements for fuel cells operating without external humidification.[54]

An early indication that side chain length affected membrane properties (e.g., proton conductivity) was observed with the short-side-chain (SSC) PFSA ionomer (i.e., a membrane with a PTFE backbone similar to Nafion but $-OCF_2CF_2SO_3H$ side chains)[55−57] first synthesized by the Dow Chemical Company.[58] Although SAXS and SANS measurements[2,56,57,59] revealed that the hydrated morphology (i.e., relative position of the ionomer peak) was quite similar to Nafion, the proton conductivity was determined to be significantly higher for membranes with EWs of approximately 800 when compared to Nafion 117.[2,59−61] This superiority was confirmed in fuel cell testing with current densities observed nearly 3 times higher at a potential of 0.5 V.[62] Recently, the SSC ionomer has experienced a resurgence of interest due to the much simpler synthesis of the base monomer by Solvay Solexis, and is thus commercially available, at a more reasonable cost than previously available, under the trade name Hyflon.[63−65] Other PFSA membranes have been synthesized that show higher proton conductivities than Nafion 117; of significance is the membrane developed by the 3M company with $-O(CF_2)_4SO_3H$ side chains using an electrochemical fluorination process.[66,67] The observed higher proton conductivities in PFSA membranes with shorter side chains than Nafion are undoubtedly linked to the higher exchange capacity but perhaps also to subtle changes to the hydrated morphology.[2,68]

There is now a substantial body of literature describing molecular modeling studies[69−97] seeking to understand the relationship between polymer architecture and transport of various species (e.g., water, protons, etc.) important to the performance of the ionomer in a fuel cell.[54] Of relevance to the current work, efforts have been aimed at elucidating how the chemistry of the side chain[69,71,80,89,91,92] affects the aggregation of the acidic groups and the dissociation and mobility of the protons. Paddison and Elliot[89,91] performed *ab initio* self-consistent field molecular orbital calculations on a single short-side-chain perfluorinated sulfonic acid segment carrying two side sulfonic acid groups, hydrated by a few additional water molecules. They investigated the effect of the spacing between the side sulfonic acid groups on the backbone of the segment on the ability of water molecules to form continuous hydrogen bonds along the segment. Their work suggests the importance of sulfonic group separation in the formation of the hydrogen bonding network in PEMs; however, they did not carry out quantitative analysis of water cluster distribution. Jang et al.[83] performed molecular dynamics to study the effect of molecular architectural variance of Nafion 117. One variance has the side chains evenly distributed along the backbone; the other has 10 side chains all placed at one end of the polymer. Their MD study showed that the PEM consisting of the end-weighted molecules gives rise to larger clusters, whereas the molecules with regularly spaced side chains give rise to smaller but more dispersed clusters.

We report on classical molecular dynamics simulations of Nafion and the SSC membrane in an effort to identify differences in hydrated morphology and the connections between morphology and the rates and mechanism of proton diffusion. The latter is, of course, limited to diffusion of hydronium ions, as our simulations do not allow for the breaking of any covalent bonds. Nevertheless, these simulations are useful in understanding how vehicular diffusion changes as a function of ionomer chemistry and hydration. Furthermore, insight is obtained on how the length of the pendant side chains affects the intracluster diffusion of water and hydronium ions, as well as the connectivity of the domains containing the water molecules and ions (i.e., H_3O^+ and $-SO_3^-$). This should prove helpful in identifying specific features of PFSA membranes that may be modified to enhance proton transport.

Molecular Models and Simulations

The chemical structures of the repeat unit (i.e., monomer) of both Nafion and the SSC PFSA membrane are shown in Figure 1. We selected a polymeric structure with the side chains separated by seven tetrafluoroethylene (i.e., $-CF_2CF_2-$) units in the backbone for both ionomers, thus allowing direct comparison with previous MD simulations involving Nafion.[98−100] This results in similar equivalent weights for each polymer: an EW of 1143 for Nafion and an EW of 977 for the SSC ionomer. This choice allows assessment of the effect of side chain length on two systems with similar backbone structure. While this

choice corresponds directly to the readily available Nafion 117 (i.e., EW ~ 1100 g/mol), the SSC ionomer in our simulations is significantly higher in EW than commonly utilized in fuel cells (e.g., EW ~ 800 g/mol). However, a recent extensive characterization study of SSC membranes allows comparison of structural and transport data with Dow membranes of 1084 EW.[2] Furthermore, the molecular-level trends observed in our simulations should be applicable to other equivalent weights.

Force fields have been developed for both Nafion[70,74,83] and the SSC PFSA membrane.[97] Both PFSA ionomers were modeled in this study as oligomers consisting of only three monomer units, resulting in fragments with 48 CF_X groups along the backbone, similarly to previous work.[98] Although these molecules are considerably shorter than those in a real ionomer (e.g., for Nafion, there are at least 90 monomer units per macromolecule), previous work[98] revealed little difference to simulations involving fragments consisting of 10 monomers. Furthermore, the oligomers have short relaxation times and are therefore easier to equilibrate. It is computationally intractable to fully relax the fragments with macromolecules of realistic molecular weight.[97] Consequently, a united atom model for the CF_X groups on both the backbone and side chains was implemented for computational efficiency using Lennard-Jones parameters developed by Cui et al.[101,102] The backbone does not carry electric charge, save for the united atom at which the side chain is attached, and interacts only via Lennard-Jones and intramolecular interactions. Bond lengths, bond angles, and partial charges were determined for the side chains from the parameters of Vishnyakov and Neimark.[74] The charge assigned to a united atom is the sum of charges from the atomistic model. The force constants for bond stretching and bond angle bending were taken from Gejji et al.[103] and Cornell et al.[104] The torsional potential was taken from Rivin et al.[105]

Intramolecular sites on the same molecule separated by more than three bonds, and sites on different molecules, also interact via nonbonded interactions, including the Lennard-Jones and electrostatic (between charged sites) interactions. Previous simulations of hydrated Nafion[98] did not include electrostatic intramolecular interactions; however, presently, they are included. The effect is slight in most cases, and the essential features of pair correlation functions are very small, except for the sulfur−sulfur pair correlation function (PCF), $g(r)$. Thus, we have included the results for the sulfur−sulfur PCFs in the present work. The other PCFs, which are only slightly modified, however, are provided in the Supporting Information.

The water was modeled using the TIP3P model[106,107] with a flexible OH bond.[104] Similar bond distances, bond angles, and the force constants were employed for the hydronium ions, H_3O^+, as were used for the water molecules, with partial charges for the oxygen and hydrogen atoms taken from Urata et al.[85] In the calculation of nonbonded interactions, the Lennard-Jones interaction was truncated using a cutoff distance of 10 Å. The electrostatic interaction was implemented with a site−site reaction field method that has proven to be accurate for modeling aqueous ionic solutions.[108,109] In this method, Coulombic interactions between charged sites were calculated within a distance of 10 Å, and the reaction field contribution was implemented with a uniform background counter charge.

The simulated systems for both PFSA membranes consisted of 64 macromolecules (i.e., a total of 192 monomers), with 192 hydronium ions (H_3O^+), the latter to ensure overall charge neutrality. The properties of each ionomer were examined for water contents corresponding to λ (defined as the number of water molecules per $-SO_3H$ group) values of 4.4, 6.4, 9.6, and 12.8. This resulted in 660, 1040, 1656, and 2272 water molecules, corresponding to 7164, 8304, 10152, and 12000 total interaction sites in the simulations. The densities and water contents were chosen on the basis of experimentally measured values for Nafion.[110] For the four levels of hydration, the experimentally determined overall densities of the system are 1.95, 1.87, 1.80, and 1.74 g/cm^3. We used a molecular volume for the SSC PFSA systems, appropriately scaled, based on the number of atoms relative to that of Nafion, keeping the molecular volume of the water and hydronium ions the same as for Nafion. All simulations were carried out at a temperature of 300 K, and data collection was performed over at least 2 ns.

Constant NVT simulations were performed for this system. The equations of motion for the interaction sites were integrated using the r-RESPA method[111] with a time step of 2.0 fs for the large time step and 0.4 fs for the intramolecular interactions. The temperature was maintained at a constant value using the Nosé−Hoover thermostat,[112−114] with a thermostat frequency of 10^{-4} fs^{-1}. The initial configurations were created by randomly placing molecular centers of all the molecules in the system on cubic lattice points within the simulation volume. Hydronium ions were initially placed without regard for the position of the sulfonate groups so as not to bias their equilibrium position. All atoms were initially assigned an infinitesimal volume by setting their corresponding Lennard-Jones parameters to null values. An MD simulation was performed for 10000 time steps in which the Lennard-Jones size parameters were gradually increased to their assigned values. Initial configurations with nonoverlapping atoms were thereby created efficiently. Equilibration using these initial configurations was then performed for at least 500 ps before any data collection was begun.

Results and Discussion

I. Visualization of the Hydrated Morphology. The morphologies of the SSC PFSA and Nafion membranes are shown in Figures 2 and 3, respectively. The snapshots are for each system at the end of the simulation at water contents corresponding to $\lambda = 4.4$ and 9.6 for parts a and b, respectively. The atoms of each ionomer have been omitted in the snapshots in order to show clearly the clustering of the water molecules. Qualitatively, the general feature for both the SSC PFSA and Nafion membranes is that of water clusters consisting of networks (either mostly disconnected, $\lambda = 4.4$ water, or mostly connected by irregularly shaped channels, $\lambda = 9.6$). At water content $\lambda = 4.4$, these figures show that the water clusters are quite small and the connectivity is poor, consistent with the findings of other authors.[94,97] The clusters are also less densely packed in the interior. At high water content, the clusters become larger and connecting channels exist between the clusters; furthermore, the water molecules in the clusters appear to be more densely packed. Both characteristics will have important effects on the long-range transport of protons and water molecules. Careful examination of the clusters also shows that most hydronium ions appear to be exposed to the exterior of the clusters, suggesting that they are lining the surface of the clusters as a result of the interaction with the oppositely charged sulfonate groups of the ionomers. However, it is also worth pointing out that both sum-frequency generation[115−117] (i.e., SFG) and second harmonic generation[118,119] (i.e., SHG) spectroscopy experiments and *ab initio* MD simulations of neat water clusters[120] and clusters of methanol and water[121] indicate the preference of hydrated protons for the surface or interface. It has been reasoned that this increased concentration of hydronium ions (or hydrated protons) is due to a dielectric mismatch at an

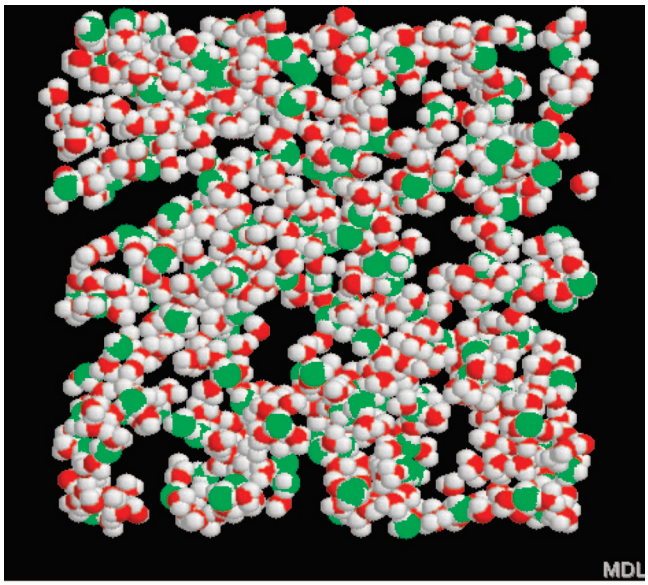

(a)

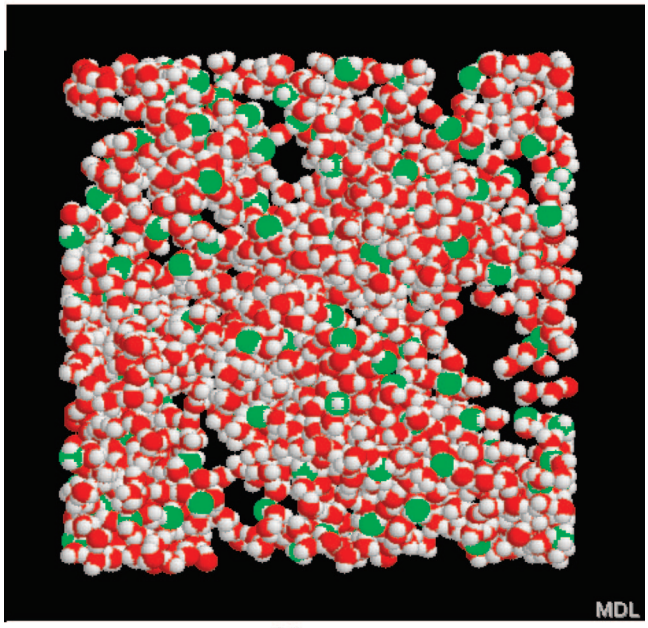

(b)

Figure 2. Snapshots of the final configurations of the SSC PFSA ionomer at hydration levels of (a) $\lambda = 4.4$ and (b) $\lambda = 9.6$. Atoms of the ionomer are not shown. Red atoms are oxygen atoms of water molecules, green atoms are oxygen atoms of hydronium ions, and white atoms are hydrogen atoms.

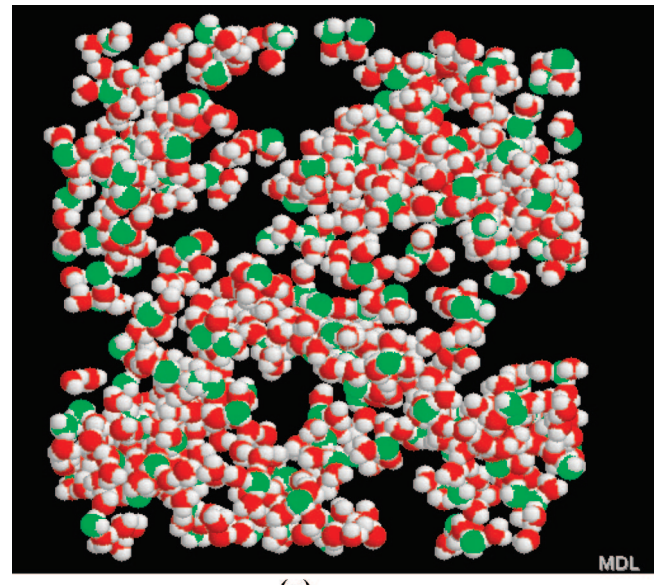

(a)

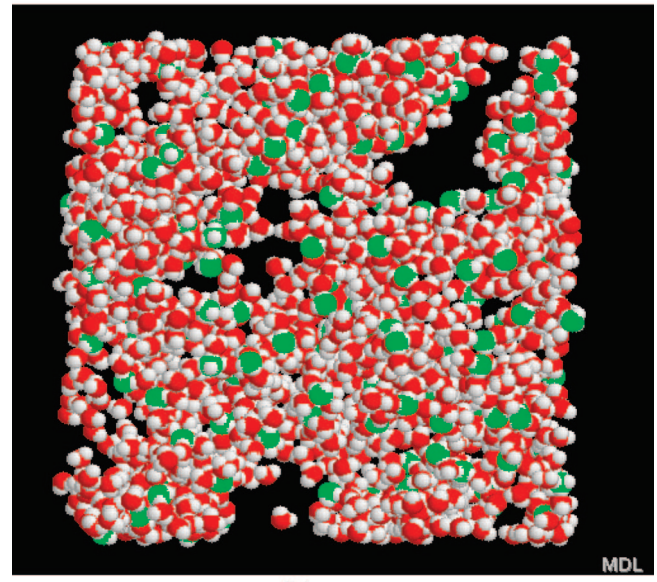

(b)

Figure 3. Snapshots of the final configurations of hydrated Nafion at hydration levels of (a) $\lambda = 4.4$ and (b) $\lambda = 9.6$. Atoms of the ionomer are not shown. The atomic color scheme is the same as that in Figure 2.

interface which is certainly the case with hydrated PFSA membranes.[122,123] Notwithstanding, a more detailed quantitative analysis of the preferential location of the hydrated protons as a function of hydration is warranted in both membranes.

II. Cluster Size Distribution and Channel Connectivity. It has been suggested from a survey of both experimental and theoretical studies of PFSA membranes that the important ingredients of proton conduction are complexity, cooperativity, and connectivity.[124] The last involves not only hydrogen bonding between the water molecules and the sulfonic acid groups and with other water molecules but importantly also hydrogen bonding between the water and ion containing domains in the polymeric matrix. Proton transport occurs through the membrane due to migration of the protons across distances several orders of magnitude larger than the size of typical clusters; thus, intercluster proton transfer has to occur, which could constitute a bottleneck in morphologies where the clusters are poorly connected. To characterize this connectivity quantitatively, we examined the cluster size distribution for water contents from $\lambda = 4.4$ to 12.8 using various critical cutoff distances, denoted by Rc. The cluster distributions were calculated by sampling the presence of certain sized clusters using a cutoff distance during the MD simulation and performing a time average. Note from the outset that the cluster distributions depend on the choice of the cutoff distance, which is somewhat arbitrary, but a comparison of the cluster structure at the same cutoff distance will show the relative tendency for cluster formation in any pair of systems. Furthermore, water molecules within the first hydration shell of a hydronium ion (i.e., less than ~3.5 Å) can make direct contact with the hydronium ions, and it is therefore possible for proton transport to occur quickly after simple ballistic motion. Thus, a cutoff distance of Rc = 3.5 Å is a reasonable critical distance based on considerations relevant to

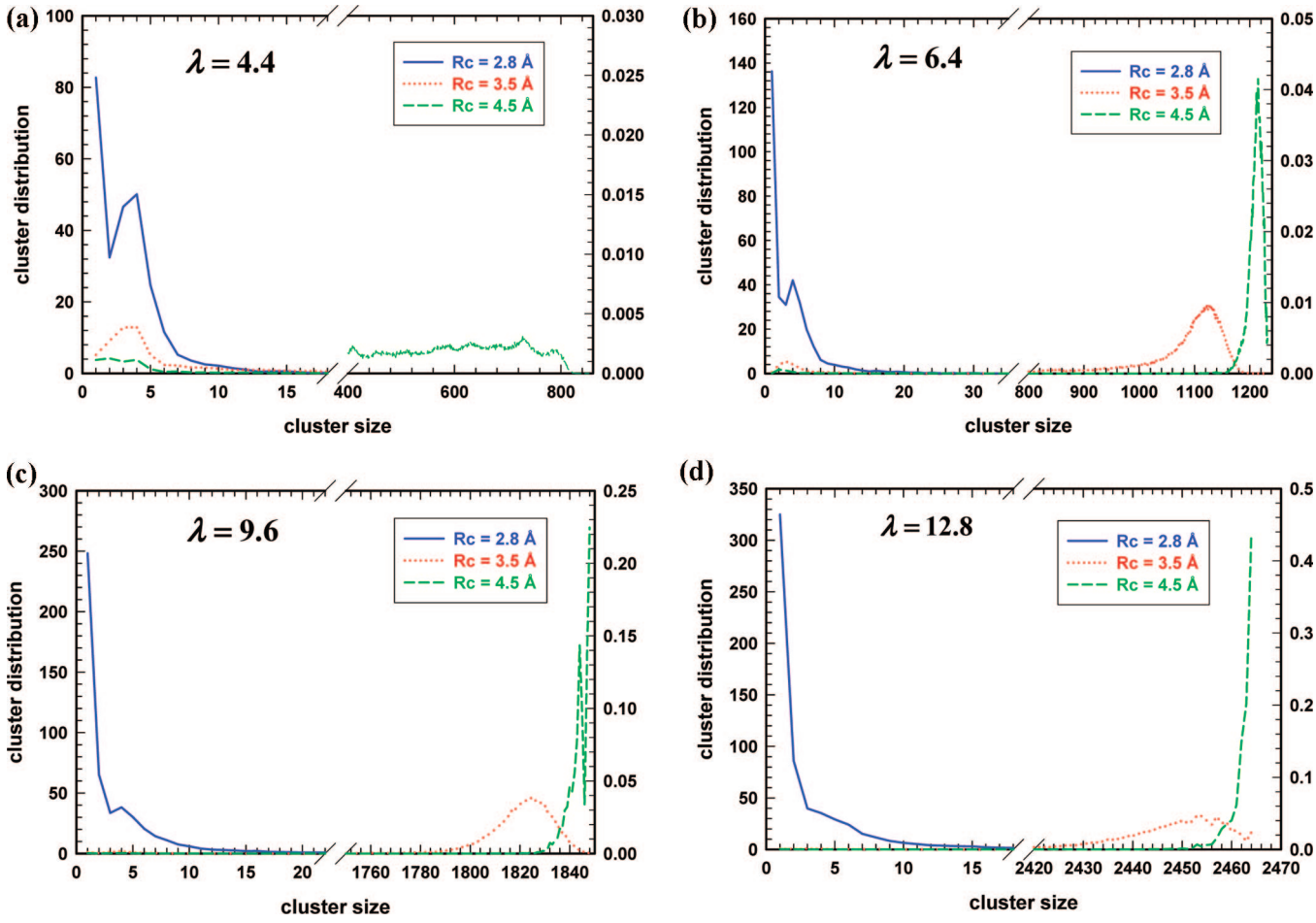

Figure 4. Cluster size distribution for hydrated SSC PFSA at water contents corresponding to (a) $\lambda = 4.4$, (b) $\lambda = 6.4$, (c) $\lambda = 9.6$, and (d) $\lambda = 12.8$.

proton transport. We have also examined other critical distances to obtain a more complete picture of the cluster connectivity.

Figures 4 and 5 display the cluster size distribution for the SSC and Nafion membranes, respectively, each at four distinct hydration levels and for three representative critical cutoff distances: Rc = 2.8 Å (corresponding to the first peak position of the water−-hydronium ion $g_{O-O}(r)$, see Figure 9 below); Rc = 3.5 Å (slightly larger than the first minimum of $g_{O-O}(r)$, inclusive of all molecules in the first hydration shell); and Rc = 4.5 Å (inclusive of the second hydration shell). The cluster size distribution represents the average number of clusters present in the system corresponding to a particular cluster size. Figure 4 indicates the presence of only small water clusters in the morphology of the SSC PFSA membrane at all water contents when a cutoff of Rc = 2.8 Å is applied. As the water content is increased, clusters of increasing size are formed, with the largest cluster size consisting of 25, 50, 100, and 200 molecules for water contents of 4.4, 6.4, 9.6, and 12.8, respectively. For Nafion with Rc = 2.8 Å, similar behavior was observed, with a maximum cluster size similar to that of the SSC PFSA membrane.

With Rc = 3.5 Å, the SSC ionomer at a water content of $\lambda = 4.4$ (Figure 4a) is composed of only small clusters, with maximum cluster size consisting of about 250 water molecules. At the next higher hydration (Figure 4b), far fewer small clusters are present, and also a small magnitude distribution around 1123 molecules is observed. Although the probability is small, the number of molecules involved is larger, representing the vast majority of the water molecules and hydronium ions in the system. Such clusters, as indicated earlier, are sample-spanning clusters (SaSC) due to the formation of connected water channels or domains throughout the system. At water contents of $\lambda = 9.6$ and 12.8, a decrease is observed both in size and in number of small clusters, while at the same time an increase is evident in the height of the peak corresponding to the SaSC.

A continuous distribution for all cluster sizes with some significant peaks for cluster sizes less than about 20 molecules is observed in the SSC PFSA ionomer at the lowest hydration for Rc = 4.5 Å. At the next higher hydration level (i.e., $\lambda = 6.4$), the appearance of the SaSC peak and at larger cluster size is again observed. Further increase of the water content to $\lambda = 9.6$ and 12.8 leads to higher peaks and a shift of the peak position to even larger clusters. There is also an observed reduction in both the number and size of the small clusters for increasing water content. This reflects the increased probability that a water molecule will find a near neighbor with increasing water content. The formation of a SaSC indicates that the entire membrane is likely to be connected with water channels that enable efficient proton conductivity. We note that a cutoff of 4.5 Å would include the second hydration shell of the water or hydronium ion. The molecules would then have to undergo vehicular diffusion to move within the first hydration shell to be in direct contact with the next molecule in the cluster, which is a slower process than the ballistic motion of molecules in the first hydration shell. Proton transfer through this route is slower.

The cluster distribution and connectivity for Nafion are qualitatively similar to that observed in a SSC PFSA membrane,

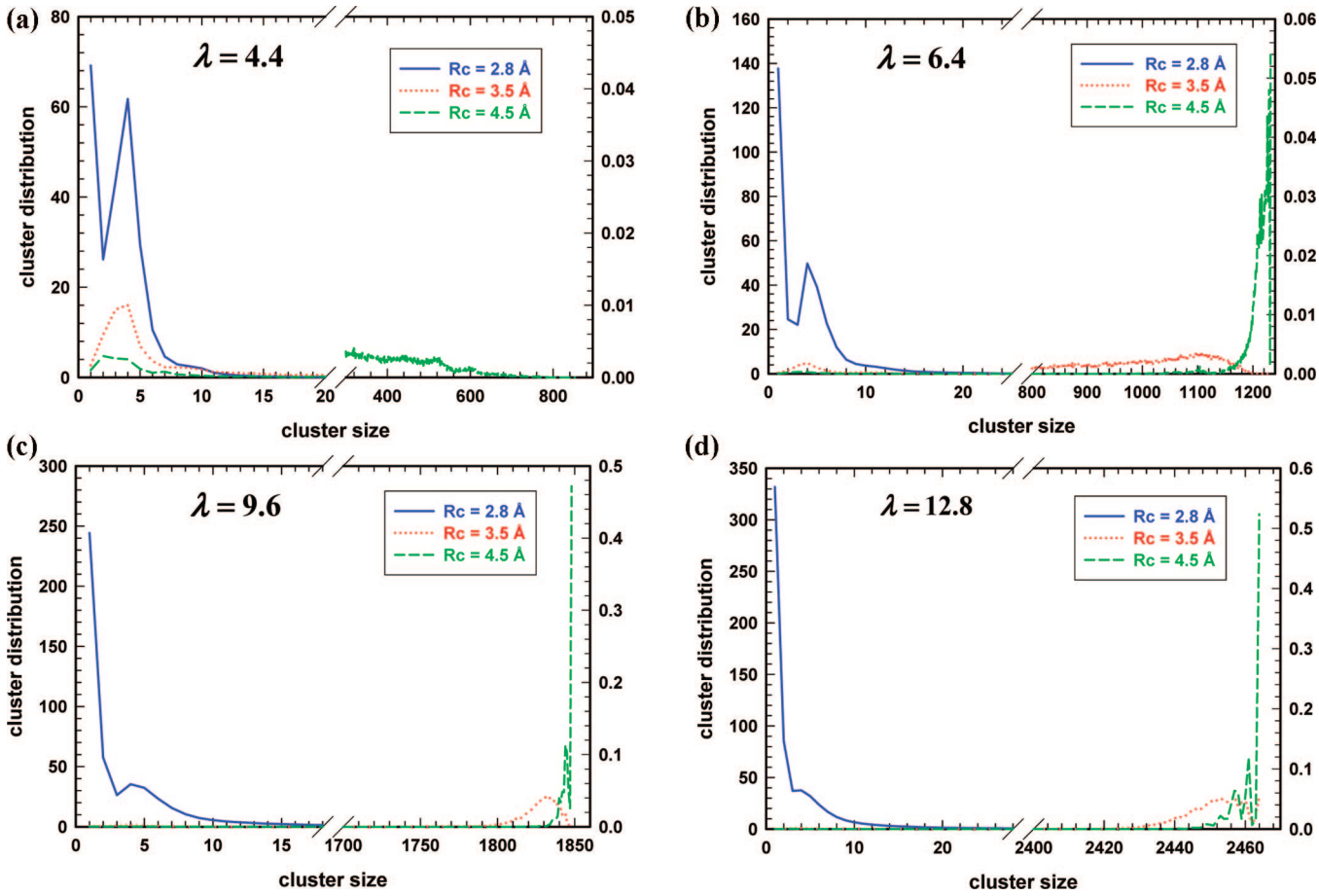

Figure 5. Cluster size distribution for hydrated Nafion at water contents corresponding to (a) $\lambda = 4.4$, (b) $\lambda = 6.4$, (c) $\lambda = 9.6$, and (d) $\lambda = 12.8$.

as inferred from Figure 5. The differences are mostly quantitative, and are more easily recognized from the cumulative number of molecules in the cluster discussed below.

The global picture of the cluster distribution and connectivity is explored in Figure 6, which displays the cumulative probability of finding a molecule in a cluster of a specific size for both PFSA membranes across the various hydration levels. The cumulative probability has been normalized for ease of comparison. For the SSC PFSA with Rc = 2.8 Å, the cumulative probability reaches a plateau at rather small cluster sizes, consistent with the fact that only small clusters are present. Hence, for both Nafion and the SSC PSFA membrane at $\lambda =$ 4.4, nearly 100% of the water molecules and hydronium ions are in clusters of not more than 20 molecules. As the water content is increased, there is a clear tendency for the curves to shift to the right, reaching plateaus at the maximum cluster size, suggesting that the clusters become larger with increasing water content. In Figure 6b, where Rc = 3.5 Å, the behavior is quite different. At the lowest water content, the cumulative probability distribution reaches a plateau at about 250 molecules. At a hydration level where $\lambda = 6.4$, there is an initial rise to about 0.1 in the cumulative probability, then an extended region of slow increase, and a rapid rise at around 1100 molecules in cluster size. This is related to the fact that a majority of the water molecules and hydronium ions are in a large cluster spanning the entire system (i.e., a SaSC). At the higher two water contents ($\lambda =$ 9.6 and 12.8), the contributions to cumulative probability are essentially due to the rise in the amount of water in the large SaSC. In Figure 6c, with Rc = 4.5 Å, water clusters become more connected. At a water content where $\lambda = 4.4$, there is a continuous rise in the cumulative probability, suggesting the presence of clusters of all sizes. However, only a small contribution in the cumulative probability due to small clusters and a sharp rise for the SaSC is observed at the intermediate hydration level ($\lambda = 6.4$). Finally, at the two highest water contents ($\lambda =$ 9.6 and 12.8), the number of molecules in small clusters is negligible and the vast majority of the molecules are in the SaSC, as reflected by the sharp lines in Figure 6c.

The rise in the cumulative probability curve for Nafion is more gradual than that for the SSC PFSA membrane for cutoffs at hydration levels where $\lambda = 4.4$ and 6.4 when cutoffs of Rc = 3.5 and 4.5 Å are used, respectively (see parts b and c of Figure 6). This would suggest that there is a greater contribution in the hydrated morphology due to small and intermediate sized water clusters in Nafion than in the SSC PFSA ionomer at these water contents. The latter has the tendency to form larger, more connected clusters, and this may be due to the stiffness of the shorter side chain.[71,91] As a result, the sulfonate groups are more widely separated in the SSC PFSA ionomer, which results in a dispersed aqueous phase. Dispersion of the $-SO_3^-$ groups can bridge the connection between clusters which would otherwise be isolated. This hypothesis is further supported through examination of the S−S pair correlation functions, discussed below.

The main characteristics of the water clusters in the two hydrated systems are summarized in Table 1. The difference is most obvious at the low water contents: for $\lambda = 4.4$ and 6.4, it is apparent that the percentage of water and hydronium ions in the SaSC is significantly higher in the SSC PFSA membrane.

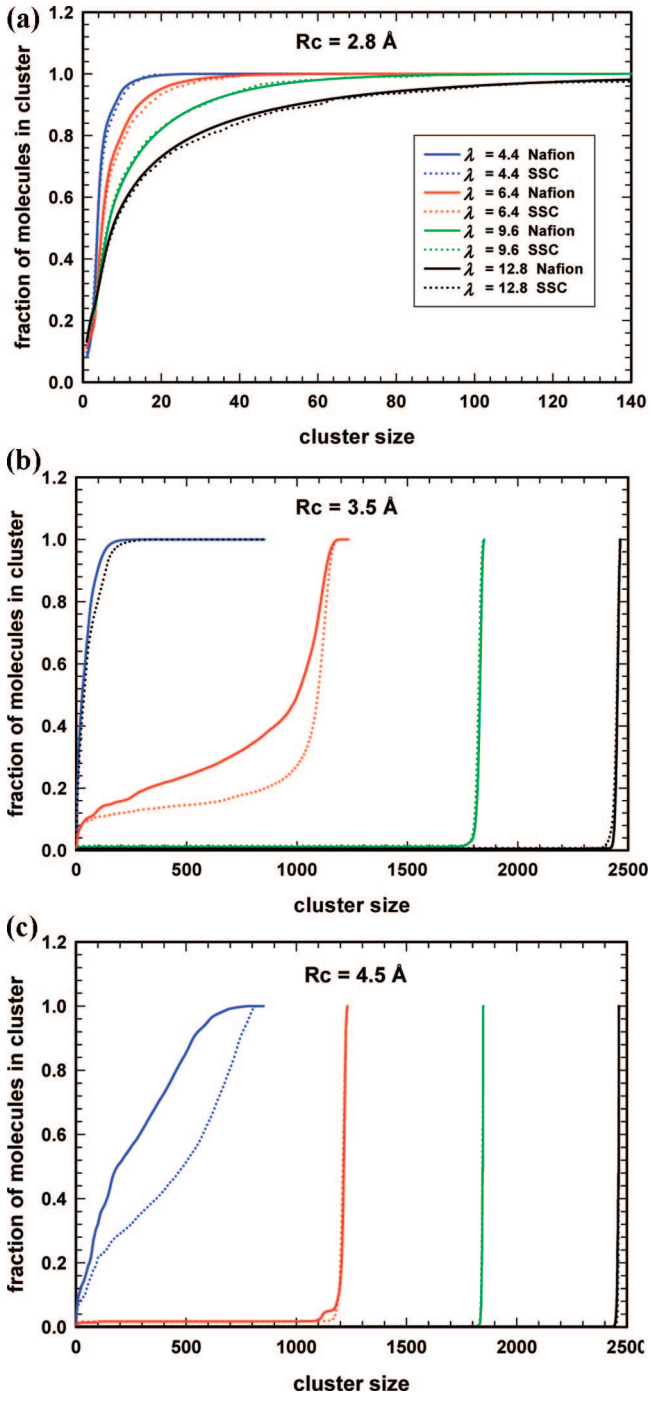

Figure 6. Cumulative number of molecules in clusters in hydrated SSC PFSA ionomer and Nafion for Rc of (a) 2.8 Å, (b) 3.5 Å, and (c) 4.5 Å. The line types in parts b and c are the same as those in part a.

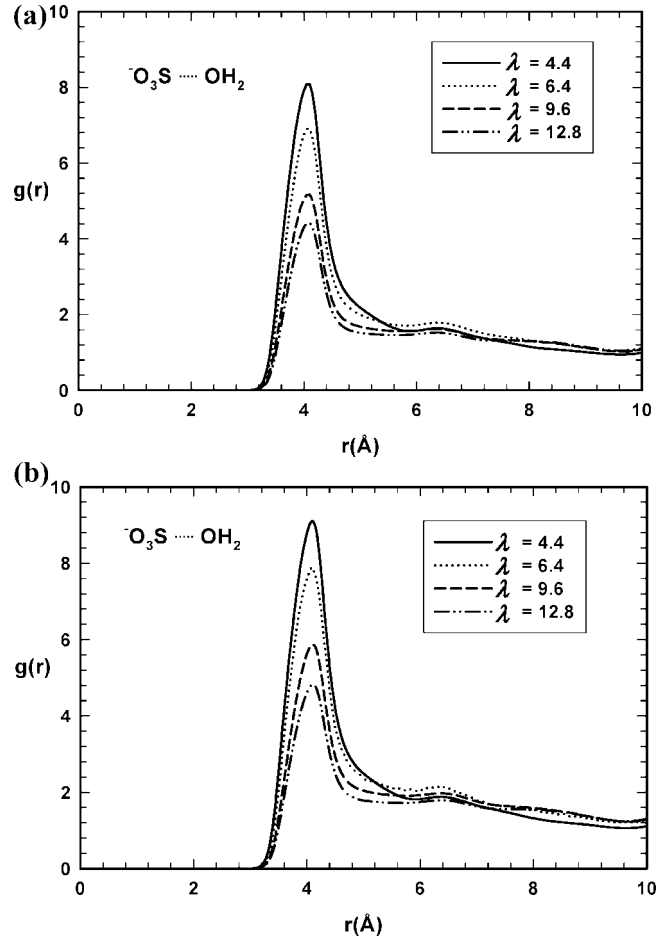

Figure 7. Sulfur−water (oxygen atom of water molecule) pair correlation functions: (a) SSC PFSA; (b) Nafion.

It is also evident that the general feature of water cluster distribution in PFSA membranes can be characterized by SaSC and its connectivity. The morphology of the aqueous phase is affected by the architecture of the PFSA ionomer. When a short cutoff distance (2.8 Å) is applied, both membranes exhibit disconnected morphologies at all water contents. For longer cutoff distances (e.g., 4.5 Å), both ionomers exhibit a single aqueous SaSC at all water contents, except the very lowest. At $\lambda = 4.4$, the water clusters in the SSC PFSA ionomer are slightly more connected than in Nafion. At intermediate cutoff distances (3.5 Å), both membranes exhibit a single aqueous SaSC at the two highest water contents and exhibit disconnected morphologies at the lowest water content. At the intermediate water content ($\lambda = 6.4$), the aqueous phase in the ionomer with the shorter side chains is again better connected than in Nafion.

III. Pair Correlation Functions. The sulfonate sulfur−water oxygen pair correlation functions are presented in Figure 7. For both PFSA membranes, the sulfur−oxygen PCF shows a strong first peak and a weak, barely visible second peak. With increasing hydration, the height of the first peak decreases. The height of the prominent peak in the PCF for the two ionomers is slightly different. For the SSC ionomer, the height of the peak is 8.2, 7.0, 5.2, and 4.4, and for Nafion, it is 9.1, 7.8, 5.9, and 4.8 at water contents of $\lambda = 4.4$, 6.4, 9.6, and 12.8, respectively. Thus, the peak is generally higher for Nafion than for the SSC PFSA membrane.

The sulfur−hydronium ion PCFs for both membranes are displayed in Figure 8 and may be compared with those for sulfur−water. The peak positions are roughly similar to those in the sulfur−water PCFs, but the heights are much greater. The dependence on water content is similar to sulfur−water; i.e., the peak height decreases with increasing water content. The height of the first peak for SSC is 15.1, 9.9, 7.0, and 5.6, and for Nafion, it is 14.2, 7.9, 5.5, and 4.4 for water contents where $\lambda = 4.4$, 6.4, 9.6, and 12.8, respectively. Thus, the height of the first peak is generally higher for the SSC ionomer than for Nafion, suggesting that the hydronium ions are, on average, more likely to be found in close proximity to the sulfonate groups in the PFSA membrane with the short side chains. This is consistent with the higher water peak in the hydrated Nafion systems, as the greater density of water molecules results in increased screening of the sulfonate anions.[88]

TABLE 1: Aqueous Cluster Characteristics as Functions of Cluster Cutoff Distance

	Rc = 2.8 Å		Rc = 3.5 Å		Rc = 4.5 Å	
	Nafion	SSC	Nafion	SSC	Nafion	SSC
$\lambda = 4.4$	N	N	N	N	Y	Y
presence of SaSC						
peak position/range	N/A	N/A	N/A	N/A	continuous distribution	continuous distribution
% molecules in SaSC	0.0	0.0	0.0	0.0	13.06	23.00
$\lambda = 6.4$	N	N	Y	Y	Y	Y
presence of SaSC						
peak position/range	N/A	N/A	1107/986−1232	1123/0−1190	1232/1159−1232	1215/1128−1232
% molecules in SaSC	0.0	0.0	41.0	74	98.36	98.21
$\lambda = 9.6$	N	N	Y	Y	Y	Y
presence of SaSC						
peak position/range	N/A	N/A	1833/1793−1848	1825/1748−1848	1848/1832−1848	1848/1820−1848
% molecules in SaSC	0.0	0.0	96.80	98.4	99.28	99.78
$\lambda = 12.8$	N	N	Y	Y	Y	Y
presence of SaSC						
peak position/range	N/A	N/A	2464/2425−2464	2453/2377−2464	2464/2445−2464	2464/2440−2464
% molecules in SaSC	0.0	0.0	99.05	99.3	99.55	99.92

The sulfur−sulfur PCFs for the SSC PFSA and Nafion membranes are displayed in Figures 9 and 10, respectively. As mentioned earlier, the inclusion of an intramolecular electrostatic interaction was expected to have only a noticeable effect on the sulfur−sulfur PCFs, mostly via the intramolecular correlation function. Comparison of the total sulfur−sulfur PCFs shows that the first peak at 4.8 Å is about 2.5 for the SSC ionomer and about 3.1 for Nafion at the lowest water content. This peak is always greater in Nafion and, as the water content is increased, broadens and eventually flattens. This suggests that the sulfonate groups in the ionomer with the longer side chains tend to aggregate closer to one another than those in the SSC membrane, perhaps due to the greater flexibility in the longer side chains. The total sulfur−sulfur PCFs are decomposed into intramolecular and intermolecular components in Figures 9b,c and 10b,c. It is apparent that, except at the lowest water content ($\lambda = 4.4$), the pair correlation function is dominated by the contribution from the intermolecular correlation. Also, for both the intermolecular and intramolecular PCFs, the first peak is higher for Nafion than for the SSC ionomer. This would again underscore the increased rigidity of the shorter side chains.

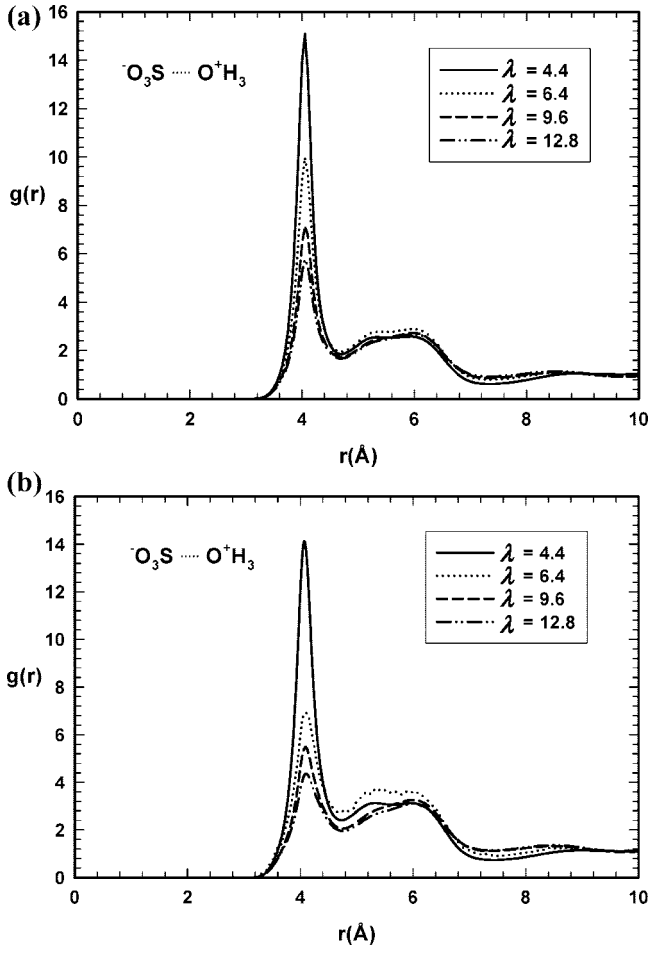

Figure 8. Sulfur−hydronium (oxygen atom of hydronium ion) pair correlation function: (a) SSC-PFSA; (b) Nafion.

Figure 11 displays the hydronium ion−hydronium ion PCFs in relation to the sulfur−sulfur PCFs. Since the hydronium ions are the counterions of the sulfonate anions, it is expected that they will be associated with the latter at low water contents, a fact that has been observed in previous classical MD simulations.[88,93,94,97] However, as the water content is increased, the hydronium ions become more separated from the sulfonate groups. The general feature of the hydronium−hydronium PCFs is that they peak at relatively large distances (i.e., >6 Å). The probability for close contact (at about 3 Å) is extremely small, and peaks in the PCFs occur at roughly about 7 and 9 Å. Clearly, repulsion prevents any close association of the hydronium ions, and due to their association with the sulfonate groups, their correlations occur at relatively great distances. The position of the peak may in some way reflect the character or size of the aqueous clusters. Small clusters (e.g., those at $\lambda = 4.4$) apparently are more likely to concentrate the hydronium ions in a small spatial region and cause stronger correlation. Furthermore, "pinning" of the H_3O^+ to one or more $-SO_3^-$ groups is likely to occur when little water is available to solvate the fixed anions.[97]

Diffusion coefficients calculated from the mean-square displacement of H_2O and H_3O^+ for both PFSA membranes at all four hydration levels are plotted in Figure 12. The results were derived from simulations of at least 2 ns in length, with a sampling time of at least 1 ns following equilibration. The numerical results are collected in Table 2, along with experimental values taken from Kreuer et al.[2,125] The simulated hydronium ion diffusion coefficients for Nafion are consistently higher than those for the SSC PFSA membranes across the entire range of hydration. The simulated values are all lower, in comparison to the experimental values, though only slightly lower at the lowest hydration level (i.e., $\lambda = 4.4$) with the SSC ionomer. This would seem to support the findings of others that,

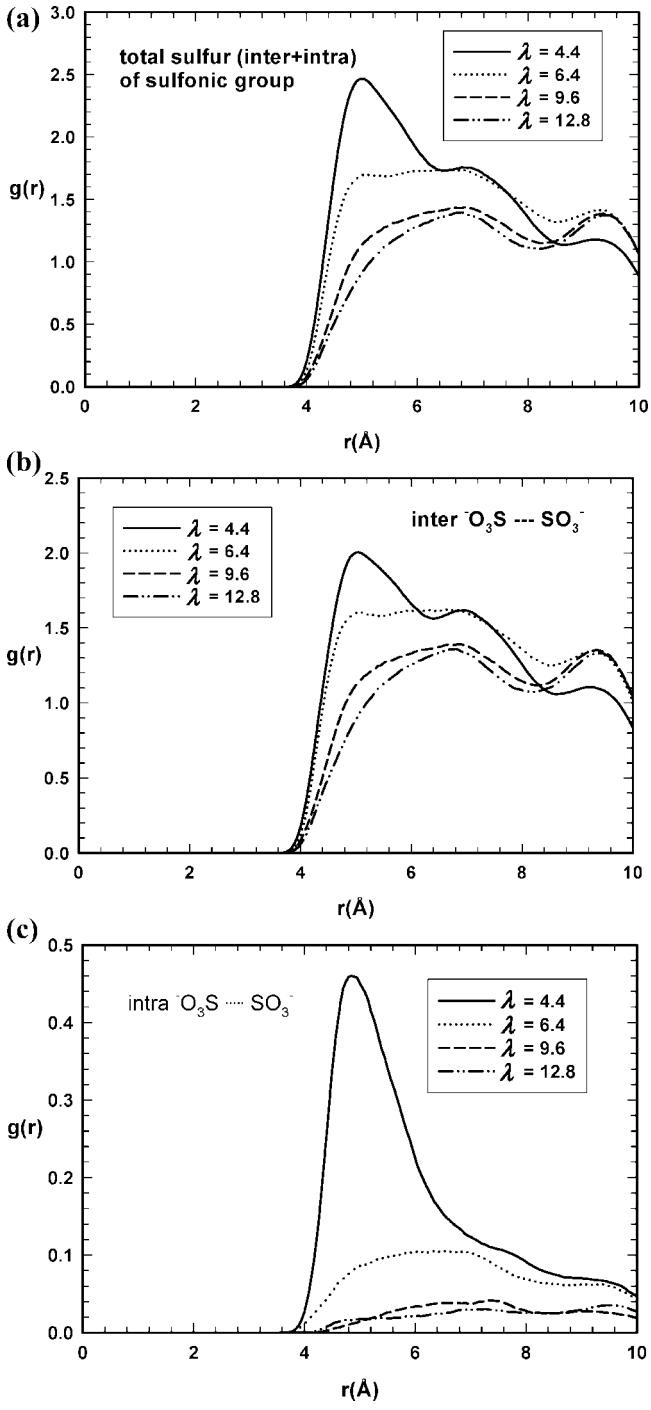

Figure 9. Sulfur−sulfur pair correlation functions for hydrated SSC PFSA ionomer: (a) total; (b) intermolecular; (c) intramolecular.

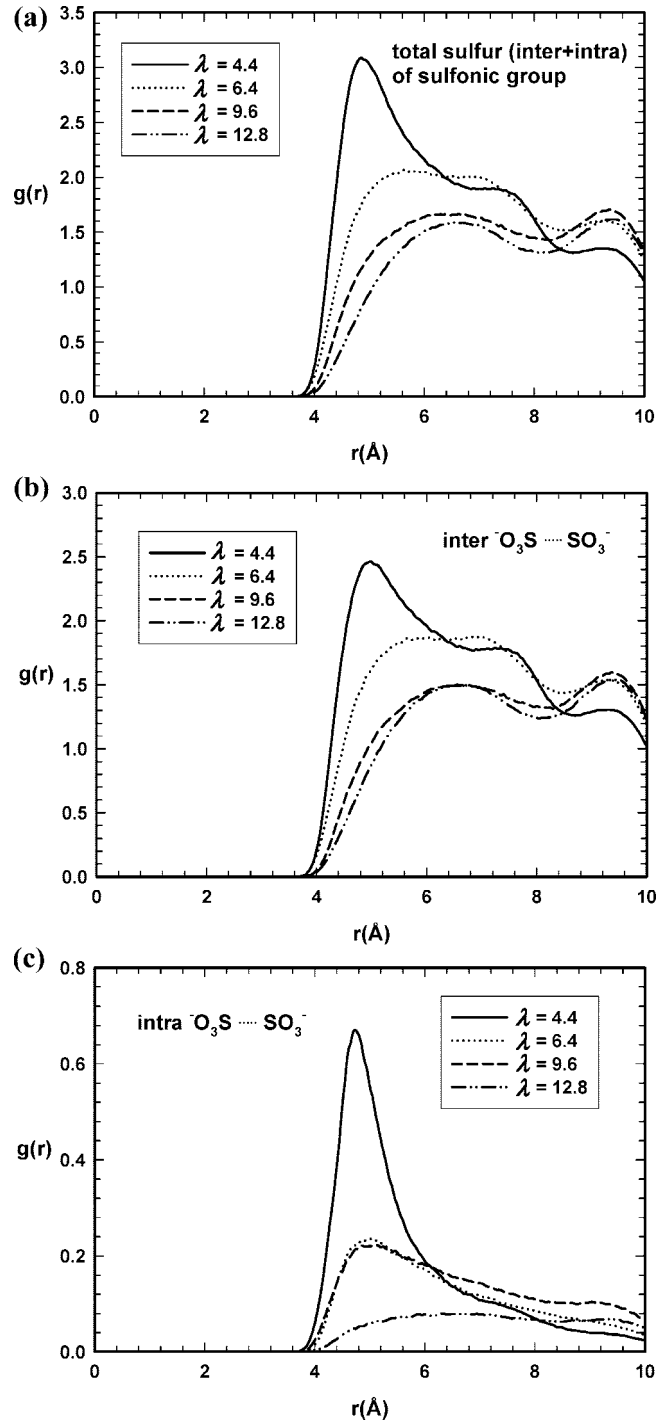

Figure 10. Sulfur−sulfur pair correlation functions for hydrated Nafion: (a) total; (b) intermolecular; (c) intramolecular.

as the water content is increased, the contribution of proton hopping to the overall proton diffusion increases. The agreement seen in the hydronium ion diffusion coefficients with measured proton diffusion coefficients does not rule out proton hopping at very low water contents, and although it has been suggested that under minimal hydration the mechanism may be vehicular (i.e., as H_3O^+),[3] it is probably more complicated than simply *en masse* diffusion. The water diffusion coefficients are also lower in the SSC ionomer at the various water contents, with the exception of $\lambda = 9.6$, where they are essentially equal. The calculated H_2O diffusion coefficients are consistently much higher than the experimental values, in contrast to the hydronium ion diffusion coefficients. This is a trend observed in the classical MD simulations of Dupuis et al.[93,95] using both a different model for Nafion and the water.

Conclusions

Molecular dynamics simulations were performed to analyze the effect of the length of the side chain on hydrated morphology and hydronium ion diffusion in Nafion and the SSC PFSA membranes. The cluster distributions displayed distinctive differences at the lower water contents ($\lambda = 4.4$ and 6.4); i.e., hydration of the SSC PFSA membrane tends to produce a more dispersed cluster distributions. At higher water content, the cluster differences between the two systems become very small,

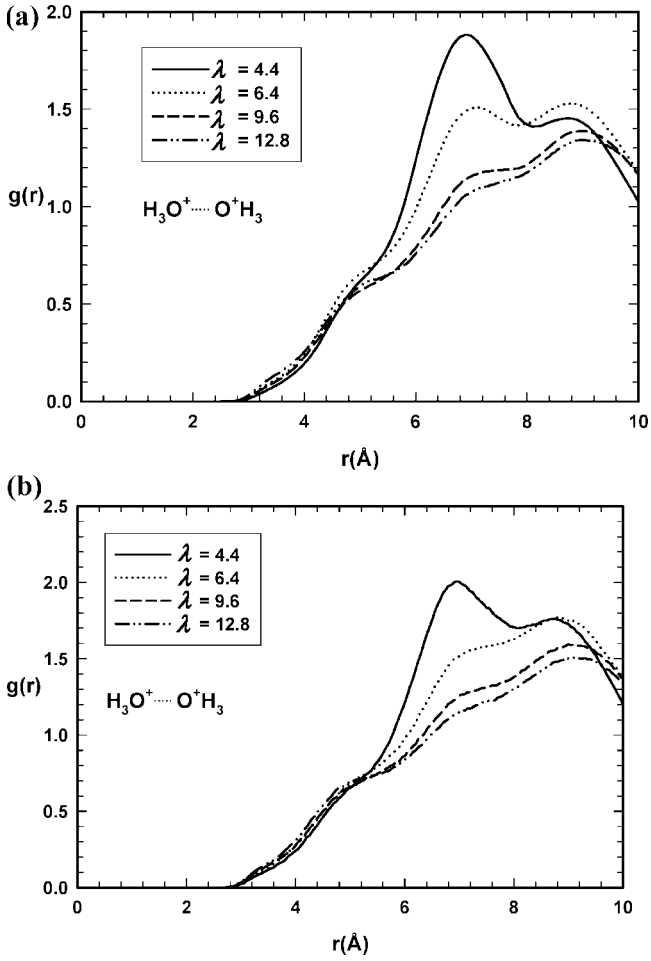

Figure 11. Hydronium ion−hydronium ion pair correlation functions for (a) SSC PFSA ionomer and (b) Nafion.

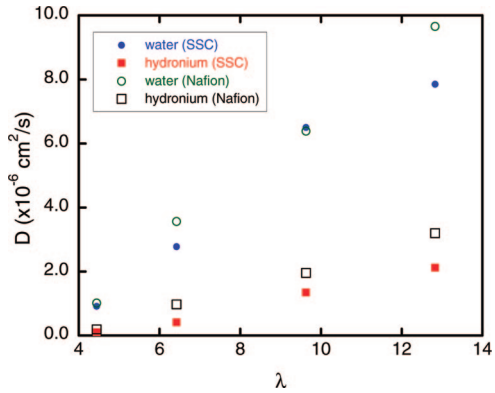

Figure 12. Water and hydronium ion diffusion coefficients of hydrated Nafion and SSC PFSA ionomers.

even though the SSC PFSA appears to show a slight tendency to be more connected. Since the hydrated membrane is inherently a heterogeneous system, even when the average water concentration is high, there are fluctuations where the local water concentration is low so that the mechanism considered here at lower water concentration is in operation. It is recognized that consideration of connectivity based on a molecular distance alone (which is the criterion used here for inclusion in a cluster) may not be discriminative enough to characterize the connectivity of a water-channel network; the channel width, for example, may also be important. A more complete method for characterizing the connectivity of a water-channel network, and a much larger system, is needed to understand completely the origin of the conductance behavior of these membrane materials. Nevertheless, an initial step has been taken in that direction, and the insight gained in this work provides a useful basis for understanding such systems. We are currently developing better methods for characterizing the water cluster-channel network and for directly calculating proton conductivity in the framework of reactive molecular dynamics.

TABLE 2: Diffusion Coefficients[a] for Water and Hydronium Ions in Hydrated SSC PFSA and Nafion Membranes at Various Water Contents

	SSC PFSA		Nafion	
water content (λ)	H_2O	H_3O^+	H_2O	H_3O^+
4.4	0.91 (0.8_5)[b]	0.11 (0.16)[b]	1.02 (0.5)[c]	0.20 (0.8)[c]
6.4	2.78 (1.4)	0.41_5 (0.9)	3.56 (2.0)	0.97 (1.8)
9.6	6.50 (4.5)	1.34 (6.0)	6.39 (4.4)	1.96 (5.0)
12.8	7.86 (5.0)	2.12 (10.0)	9.66 (5.2)	3.20 (9.0)

[a] Calculated from mean-square displacements. All values $\times 10^{-6}$ $cm^2\ s^{-1}$. [b] Values in parentheses for both water and hydrated proton for the SSC PFSA membrane are experimental values of the Dow membrane with an EW of 1150.[3] [c] Values in parentheses for both water and hydrated proton for the Nafion membrane are experimental values for Nafion 117.[118]

The simulations indicate that the SSC PFSA tends to induce more dispersed water cluster distribution, and thus enhance the connectivity of the clusters by water channels, whereas the Nafion, with a longer and more flexible side chain, is more amenable to aggregate and form clusters that are more disconnected than the SSC PFSA. We also examined various pair correlation functions of which the most relevant are the ones that involve the sulfonic acid group and the hydronium ion. The pair correlation functions also suggest a more dispersed water distribution in the SSC PFSA membranes than Nafion, as indicated by lower peaks in the sulfur−sulfur and hydronium−hydronium PCFs, consistent with cluster distribution analysis. The diffusion coefficient of water and hydronium ions are both slightly lower in the SSC PFSA membrane when compared to Nafion, suggesting that structural diffusion by proton hopping may account for the observed higher conductivities in the SSC PFSA membrane.

Acknowledgment. This work was supported by a grant from the U.S. Department of Energy BES program under Contract No. DE-FG02-05ER15723. Resources of the Center for Computational Sciences at Oak Ridge National Laboratory, which is supported by the Office of Science of the DOE under Contract DE-AC05-00OR22725, were used through the University of Tennessee Computational Science Initiative.

Supporting Information Available: Further analysis in the form of hydration histograms and radial distribution functions are provided. This information is available free of charge via the Internet at http://pubs.acs.org.

References and Notes

(1) Paddison, S. J. *Annu. Rev. Mater. Res.* **2003**, *33*, 289.

(2) Kreuer, K. D.; Schuster, M.; Obliers, B.; Diat, O.; Traub, U.; Fuchs, A.; Klock, U.; Paddison, S. J.; Maier, J. *J. Power Sources* **2008**, *178*, 499.

(3) Kreuer, K. D.; Paddison, S. J.; Spohr, E.; Schuster, M. *Chem. Rev.* **2004**, *104*, 4637.

(4) Elliott, J. A.; Paddison, S. J. *Phys. Chem. Chem. Phys.* **2007**, *9*, 2602.

(5) Tuckerman, M.; Laasonen, K.; Sprik, M.; Parrinello, M. *J. Phys. Chem.* **1995**, *99*, 5749.

(6) Marx, D.; Tuckerman, M. E.; Hutter, J.; Parrinello, M. *Nature* **1999**, *397*, 601.
(7) Agmon, N. *Chem. Phys. Lett.* **1995**, *244*, 456.
(8) Lapid, H.; Agmon, N.; Petersen, M. K.; Voth, G. A. *J. Chem. Phys.* **2005**, *122*, 014506.
(9) Kreuer, K. D. *Solid State Ionics* **2000**, *136*, 149.
(10) Eisenberg, A. *Macromolecules* **1970**, *3*, 147.
(11) Gierke, T. D.; Munn, G. E.; Wilson, F. C. *J. Polym. Sci.* **1981**, *19*, 1687.
(12) Gebel, G.; Lambard, J. *Macromolecules* **1997**, *30*, 7914.
(13) Litt, M. H. *Polym. Prepr.* **1997**, *38*, 80.
(14) Haubold, H. G.; Vad, T.; Jungbluth, H.; Hiller, P. *Electrochim. Acta* **2001**, *46*, 1559.
(15) Rollet, A. L.; Diat, O.; Gebel, G. *J. Phys. Chem. B* **2002**, *106*, 3033.
(16) Rubatat, L.; Rollet, A. L.; Gebel, G.; Diat, O. *Macromolecules* **2002**, *35*, 4050.
(17) Kreuer, K. D. *J. Membr. Sci.* **2001**, *185*, 29.
(18) Schmidt-Rohr, K.; Chen, Q. *Nat. Mater.* **2008**, *7*, 75.
(19) Falk, M. *Can. J. Chem.* **1980**, *58*, 1495.
(20) Duplessix, R.; Escoubes, M.; Rodmacq, B.; Volino, F.; Roche, E.; Eisenberg, A.; Pineri, M. In *Water in Polymers*; Rowland, S. P., Ed.; American Chemical Society: Washington, DC, 1980.
(21) Rodmacq, B.; Coey, J. M.; Escoubes, M.; Roche, E.; Duplessix, R.; Eisenberg, A.; Pineri, M. In *Water in Polymers*; Rowland, S. P., Ed.; American Chemical Society: Washington, DC, 1980.
(22) Gierke, T. D.; Munn, G. E.; Wilson, F. C. *J. Polym. Sci., Part B: Polym. Phys.* **1981**, *19*, 1687.
(23) Hsu, W. Y.; Gierke, T. D. *J. Membr. Sci.* **1983**, *13*, 307.
(24) Yeager, H. L.; Steck, A. *J. Electrochem. Soc.* **1981**, *128*, 1880.
(25) Verbrugge, M. W.; Hill, R. F. *J. Electrochem. Soc.* **1990**, *137*, 886.
(26) Gebel, G. *Polymer* **2000**, *41*, 5829.
(27) James, P. J.; Elliott, J. A.; McMaster, T. J.; Newton, J. M.; Elliott, A. M. S.; Hanna, S.; Miles, M. J. *J. Mater. Sci.* **2000**, *35*, 5111.
(28) Rollet, A. L.; Gebel, G.; Simonin, J. P.; Turq, P. *J. Polym. Sci., Part B: Polym. Phys.* **2001**, *39*, 548.
(29) Young, S. K.; Trevino, S. F.; Tan, N. C. B. *J. Polym. Sci., Part B: Polym. Phys.* **2002**, *40*, 387.
(30) Fujimura, M.; Hashimoto, T.; Kawai, H. *Macromolecules* **1981**, *14*, 1309.
(31) Fujimura, M.; Hashimoto, T.; Kawai, H. *Macromolecules* **1982**, *15*, 136.
(32) Roche, E. J.; Pineri, M.; Duplessix, R.; Levelut, A. M. *J. Polym. Sci., Part B: Polym. Phys.* **1981**, *19*, 1.
(33) Heaney, M. D.; Pellegrino, J. *J. Membr. Sci.* **1989**, *47*, 143.
(34) Lehmani, A.; Durand-Vidal, S.; Turq, P. *J. Appl. Polym. Sci.* **1998**, *68*, 503.
(35) Porat, Z.; Fryer, J. R.; Huxham, M.; Rubinstein, I. *J. Phys. Chem.* **1995**, *99*, 4667.
(36) Eikerling, M.; Kornyshev, A. A.; Stimming, U. *J. Phys. Chem. B* **1997**, *101*, 10807.
(37) Datye, V. K.; Taylor, P. L.; Hopfinger, A. J. *Macromolecules* **1984**, *17*, 1704.
(38) Mauritz, K. A.; Hora, C. J.; Hopfinger, A. J. In *Ions in Polymers*; Eisenberg, A., Ed.; American Chemical Society: Washington, DC, 1980.
(39) Mauritz, K. A.; Rogers, C. E. *Macromolecules* **1985**, *18*, 483.
(40) Dreyfus, B. *Macromolecules* **1985**, *18*, 284.
(41) Elliott, J. A.; Hanna, S.; Elliott, A. M. S.; Cooley, G. E. *Macromolecules* **2000**, *33*, 4161.
(42) Tovbin, Y. K. *Zh. Fiz. Khim.* **1998**, *72*, 55.
(43) Tovbin, Y. K.; Vasyatkin, N. F. *Colloids Surf., A* **1999**, *158*, 385.
(44) Cui, S. T.; Liu, J. W.; Selvan, M. E.; Keffer, D. J.; Edwards, B. J.; Steele, W. V. *J. Phys. Chem. B* **2007**, *111*, 2208.
(45) Tuckerman, M.; Laasonen, K.; Sprik, M.; Parrinello, M. *J. Chem. Phys.* **1995**, *103*, 150.
(46) Schmitt, U. W.; Voth, G. A. *J. Chem. Phys.* **1999**, *111*, 9361.
(47) Doi, M.; Edwards, S. F. *The Theory of Polymer Dynamics*; Oxford University Press: Clarendon, Oxford, U.K., 1986.
(48) Savadogo, O. *J. New Mater. Electrochem. Syst.* **1998**, *1*, 47.
(49) Kerres, J. A. *J. Membr. Sci.* **2001**, *185*, 3.
(50) Souzy, R.; Ameduri, B. *Prog. Polym. Sci.* **2005**, *30*, 644.
(51) Roziere, J.; Jones, D. J. *Annu. Rev. Mater. Res.* **2003**, *33*, 503.
(52) Alberti, G.; Casciola, M. *Annu. Rev. Mater. Res.* **2003**, *33*, 129.
(53) Savadogo, O. *J. Power Sources* **2004**, *127*, 135.
(54) Hamrock, S. J.; Yandrasits, M. A. *Polym. Rev.* **2006**, *46*, 219.
(55) Tant, M. R.; Darst, K. P.; Lee, K. D.; Martin, C. W. *Multiphase Polymers: Blends and Ionomers*; ACS Proceedings Series; American Chemical Society: Washington, DC, 1989.
(56) Moore, R. B.; Martin, C. R. *Macromolecules* **1989**, *22*, 3594.
(57) Gebel, G.; Moore, R. B. *Macromolecules* **2000**, *33*, 4850.
(58) Ezzell, B. R.; Carl, W. P.; Mod, W. A. *Sulfonic acid electrolyte cell having fluorinated polymer membrane with hydration product less than 22,000*; The Dow Chemical Company: U.S., 1982.
(59) Halim, J.; Büchi, F. N.; Haas, O.; Stamm, M.; Scherer, G. G. *Electrochim. Acta* **1994**, *39*, 1303.
(60) Zawodzinski, T. A.; Springer, T. E.; Davey, J.; Jestel, R.; Lopez, C.; Valerio, J.; Gottesfeld, S. *J. Electrochem. Soc.* **1993**, *140*, 1981.
(61) Edmondson, C. A.; Fontanella, J. J. *Solid State Ionics* **2002**, *152*, 355.
(62) Prater, K. *J. Power Sources* **1990**, *29*, 239.
(63) Arcella, V.; Ghielmi, A.; Tommasi, G. *Ann. N.Y. Acad. Sci.* **2003**, *984*, 226.
(64) Arcella, V.; Troglia, C.; Ghielmi, A. *Ind. Eng. Chem. Res.* **2005**, *44*, 7646.
(65) Ghielmi, A.; Vaccarono, P.; Troglia, C.; Arcella, V. *J. Power Sources* **2005**, *145*, 108.
(66) Hamrock, S. J.; Rivard, L. M.; Moore, G. I.; Freemeyer, H. T. *Polymer Electrolyte Membranes*, US Patent, 2004.
(67) Emery, M.; Guerra, M.; Haugen, G.; Hintzer, K.; Lochhaas, K. H.; Pham, P.; Pierpont, D.; Schaberg, M.; Thaler, A.; Yandrasits, M.; Hamrock, S. *ECS Trans.* **2007**, *11*, 3.
(68) Wu, D.; Paddison, S. J.; Elliott, J. A. *Energy Environ. Sci.* **2008**, *1*, 284.
(69) Paddison, S. J.; Zawodzinski, T. A. *Solid State Ionics* **1998**, *115*, 333.
(70) Elliott, J. A.; Hanna, S.; Elliott, A. M. S.; Cooley, G. E. *Phys. Chem. Chem. Phys.* **1999**, *1*, 4855.
(71) Paddison, S. J.; Pratt, L. R.; Zawodzinski, T. A. *J. New Mater. Electrochem. Syst.* **1999**, *2*, 183.
(72) Paddison, S. J.; Paul, R.; Zawodzinski, T. A. *J. Electrochem. Soc.* **2000**, *147*, 617.
(73) Vishnyakov, A.; Neimark, A. V. *J. Phys. Chem. B* **2000**, *104*, 4471.
(74) Vishnyakov, A.; Neimark, A. V. *J. Phys. Chem. B* **2001**, *105*, 7830.
(75) Vishnyakov, A.; Neimark, A. V. *J. Phys. Chem. B* **2001**, *105*, 9586.
(76) Paddison, S. J.; Paul, R.; Zawodzinski, T. A. *J. Chem. Phys.* **2001**, *115*, 7753.
(77) Paddison, S. J. *J. New Mater. Electrochem. Syst.* **2001**, *4*, 197.
(78) Spohr, E.; Commer, P.; Kornyshev, A. A. *J. Phys. Chem. B* **2002**, *106*, 10560.
(79) Commer, P.; Cherstvy, A. G.; Spohr, E.; Kornyshev, A. A. *Fuel Cells* **2002**, *2*, 127.
(80) Eikerling, M.; Paddison, S. J.; Zawodzinski, T. A. *J. New Mater. Electrochem. Syst.* **2002**, *5*, 15.
(81) Paddison, S. J.; Paul, R.; Kreuer, K. D. *Phys. Chem. Chem. Phys.* **2002**, *4*, 1151.
(82) Paddison, S. J.; Paul, R. *Phys. Chem. Chem. Phys.* **2002**, *4*, 1158.
(83) Jang, S. S.; Molinero, V.; Cagin, T.; Goddard, W. A. *J. Phys. Chem. B* **2004**, *108*, 3149.
(84) Paul, R.; Paddison, S. J. *J. Phys. Chem. B* **2004**, *108*, 13231.
(85) Urata, S.; Irisawa, J.; Takada, A.; Shinoda, W.; Tsuzuki, S.; Mikami, M. *J. Phys. Chem. B* **2005**, *109*, 4269.
(86) Urata, S. I., J.; Takada, A.; Shinoda, W.; Tsuzuki, S.; Mikami, M. *J. Phys. Chem. B* **2005**, *109*, 17274.
(87) Blake, N. P.; Petersen, M. K.; Voth, G. A.; Metiu, H. *J. Phys. Chem. B* **2005**, *109*, 24244.
(88) Paul, R.; Paddison, S. J. *J. Chem. Phys.* **2005**, *123*, 224704.
(89) Paddison, S. J.; Elliott, J. A. *J. Phys. Chem. A* **2005**, *109*, 7583.
(90) Petersen, M. K.; Voth, G. A. *J. Phys. Chem. B* **2006**, *110*, 18594.
(91) Paddison, S. J.; Elliott, J. A. *Phys. Chem. Chem. Phys.* **2006**, *8*, 2193.
(92) Paddison, S. J.; Elliott, J. A. *Solid State Ionics* **2006**, *177*, 2385.
(93) Venkatnathan, A.; Devanathan, R.; Dupuis, M. *J. Phys. Chem. B* **2007**, *111*, 7234.
(94) Devanathan, R.; Venkatnathan, A.; Dupuis, M. *J. Phys. Chem. B* **2007**, *111*, 8069.
(95) Devanathan, R.; Venkatnathan, A.; Dupuis, M. *J. Phys. Chem. B* **2007**, *111*, 13006.
(96) Paddison, S. J.; Elliott, J. A. *Solid State Ionics* **2007**, *178*, 561.
(97) Hristov, I. H.; Paddison, S. J.; Paul, R. *J. Phys. Chem. B* **2008**, *112*, 2937.
(98) Cui, S. T.; Liu, J.; Esai Selvan, M.; Keffer, D. J.; Edwards, B. J.; Steele, W. V. *J. Phys. Chem. B* **2007**, *111*, 2208.
(99) Selvan, M. E.; Liu, J.; Keffer, D. J.; Cui, S.; Edwards, B. J.; Steele, W. V. *J. Phys. Chem. C* **2008**, *112*, 1975.
(100) Liu, J.; Selvan, M. E.; Cui, S.; Edwards, B. J.; Keffer, D. J.; Steele, W. V. *J. Phys. Chem. C* **2008**, *112*, 1985.
(101) Cui, S. T.; Siepmann, J. I.; Cochran, H. D.; Cummings, P. T. *Fluid Phase Equilib.* **1998**, *146*, 51.
(102) Li, H.-C.; McCabe, C.; Cui, S. T.; Cummings, P. T.; Cochran, H. D. *Mol. Phys.* **2003**, *101*, 2157.

(103) Gejji, S. P.; Hermansson, K.; Lindgren, J. *J. Phys. Chem.* **1993**, *97*, 3712.
(104) Cornell, W. D.; Cieplak, P.; Bayly, C. I.; Gould, i. R.; Nerz; J, K. M.; Ferguson, D. M.; Spellmeyer, D. C.; Fox, T.; Caldwell, J. W.; Kollman, P. A. *J. Am. Chem. Soc.* **1995**, *117*, 5179.
(105) Rivin, D.; Meermeier, G.; Schneider, N. S.; Vishnyakov, A.; Neimark, A. V. *J. Phys. Chem. B* **2004**, *108*, 8900.
(106) Jorgensen, W.L.; J.; Chandrasekhar, J.; Madura, J. D.; Impey, R. W.; Klein, M. L. *J. Chem. Phys.* **1983**, *79*, 926.
(107) Price, D. J.; Brooks, C. L. *J. Chem. Phys.* **2004**, *121*, 10096.
(108) Hummer, G.; Soumpasis, D. M.; Neumann, M. *Mol. Phys.* **1992**, *77*, 769.
(109) Cui, S. T.; Harris, J. G. *Chem. Eng. Sci.* **1994**, *49*, 2749.
(110) Morris, D. R.; Sun, X. *J. Appl. Polym. Sci.* **1993**, *50*, 1445.
(111) Tuckerman, M.; Berne, B. J.; Martyna, G. J. *J. Chem. Phys.* **1992**, *97*, 1990.
(112) Nosé, S. *Mol. Phys.* **1984**, *52*, 255.
(113) Nosé, S. *J. Chem. Phys.* **1984**, *81*, 511.
(114) Hoover, W. G. *Phys. Rev. A* **1985**, *31*, 1695.
(115) Radüge, C.; Pflumio, V.; Shen, Y. R. *Chem. Phys. Lett.* **1997**, *274*, 140.
(116) Miranda, P. B.; Shen, Y. R. *J. Phys. Chem. B* **1999**, *103*, 3292.
(117) Shultz, M. S.; Baldelli, S.; Schnitzer, C.; Simonelli, D. *J. Phys. Chem. B* **2002**, *106*, 5313.
(118) Petersen, P. B.; Saykally, R. J. *J. Phys. Chem. B* **2005**, *109*, 7976.
(119) Petersen, P. B.; Saykally, R. J. *Chem. Phys. Lett.* **2008**, *458*, 255.
(120) Iyengar, S. S.; Day, T. J. F.; Voth, G. A. *Int. J. Mass Spectrosc.* **2005**, *241*, 197.
(121) Morrone, J. A.; Haslinger, K. E.; Tuckerman, M. E. *J. Phys. Chem. B* **2006**, *110*, 3712.
(122) Paddison, S. J.; Bender, G.; Kreuer, K. D.; Nicoloso, N.; Zawodzinski, T. A. *J. New Mater. Electrochem. Syst.* **2000**, *3*, 291.
(123) Paul, R.; Paddison, S. J. *Solid State Ionics* **2004**, *168*, 245.
(124) *Device and Materials Modeling in PEM Fuel Cells*; Paddison, S. J., Promislow, K. S., Eds.; Springer: New York, 2008.
(125) Kreuer, K. D. *Solid State Ionics* **1997**, *97*, 1.

JP8039803